Supplement of Biogeosciences, 16, 347–367, 2019
https://doi.org/10.5194/bg-16-347-2019-supplement

Biogeosciences
Open Access

Supplement of

Modeling oceanic nitrate and nitrite concentrations and isotopes using a 3-D inverse N cycle model

Taylor S. Martin et al.

Correspondence to: Karen L. Casciotti (kcasciotti@stanford.edu)

Section S1

Linearization of transfer function for sedimentary denitrification

This section expands on the transformations applied to the non-linear transfer function for sedimentary denitrification presented by Bohlen et al. (2012) in order to use the transfer function in our linear N cycle model. The original function is as follows:

1. DIN loss = $(0.60 + 0.19*0.99^{(O2-NO3)bottom})$*RRPOC   for water depths >= 1000m
2. DIN loss = $0.73*(0.60 + 0.19*0.99^{(O2-NO3)bottom})$*RRPOC   for water depths < 1000m

The calculation of the rain rate of particulate organic carbon (RRPOC) follows the Martin curve is as described in Text S4 (Equation 20). $(O_2\text{-}NO_3^-)_{bottom}$ is the difference between $[O_2]$ and $[NO_3^-]$ at the bottom of the water column, where it interfaces with the sediments.

For every model grid box, the depth is taken to be the depth at the bottom of the box. Each box is then assigned a multiplier of 1 (if depth >= 1000m) or 0.73 (if depth < 1000m) that will be multiplied by the sedimentary denitrification terms.

The next step is linearizing the (DIN loss)/RRPOC data presented by Bohlen et al. (2012) with respect to $(O_2\text{-}NO_3^-)_{bottom}$, since we cannot use the exponential equation in our linear system. This was performed by selecting two $(O_2\text{-}NO_3^-)_{bottom}$ cutoff points (29 µM and 141 µM), breaking the data into three groups. A piecewise linear regression was then performed on each of these sections (Figure S1), resulting in the following equations:

3. (DIN loss)/RRPOC = $0.297 – 0.005(O_2\text{-}NO_3^-)_{bottom}$ $(O_2\text{-}NO_3^-)_{bottom} <= 29$ µM
4. (DIN loss)/RRPOC = $0.222 – 0.001(O_2\text{-}NO_3^-)_{bottom}$ 29 µM < $(O_2\text{-}NO_3^-)_{bottom} <= 141$ µM
5. (DIN loss)/RRPOC = $0.105 – 0.000006(O_2\text{-}NO_3^-)_{bottom}$ 141 µM < $(O_2\text{-}NO_3^-)_{bottom}$

These $(O_2\text{-}NO_3^-)_{bottom}$ cutoff points were then converted to O_2 cutoff points in order to use a simple N-independent mask to determine which of the relationships to apply to a given model grid box. A linear relationship between $[O_2]$ and $(O_2\text{-}NO_3^-)_{bottom}$ was determined using The 2013 World Ocean Atlas interpolated data product for $[O_2]$ and $[NO_3^-]$ (Garcia et al., 2014). The linear relationship is as follows and is also shown in Figure S2:

6. $(O_2\text{-}NO_3^-)_{bottom} = 1.12[O_2]_{bottom} -55.6$

The $(O_2\text{-}NO_3^-)_{bottom}$ cutoff points can then be expressed in $[O_2]$ units as 75 and 175 µM.

The final step in modifying this transfer function for use in the linear model is to break the piecewise linear equations into a component that is dependent on N and a component that is independent of N. This facilitates the implementation of the equations in our linear system.

7. Independent + dependent = (DIN loss)/RRPOC

8. Independent = $0.297 - 0.005[O_2]$ $O_2 <= 75\ \mu M$
9. Dependent = $0.005[NO_3^-]$

10. Independent = $0.222 - 0.001[O_2]$ $75\ \mu M < O_2 <= 175\ \mu M$
11. Dependent = $0.001[NO_3^-]$

12. Independent = $0.105 - 0.000006[O_2]$ $175\ \mu M < O_2$
13. Dependent = $0.000006[NO_3^-]$

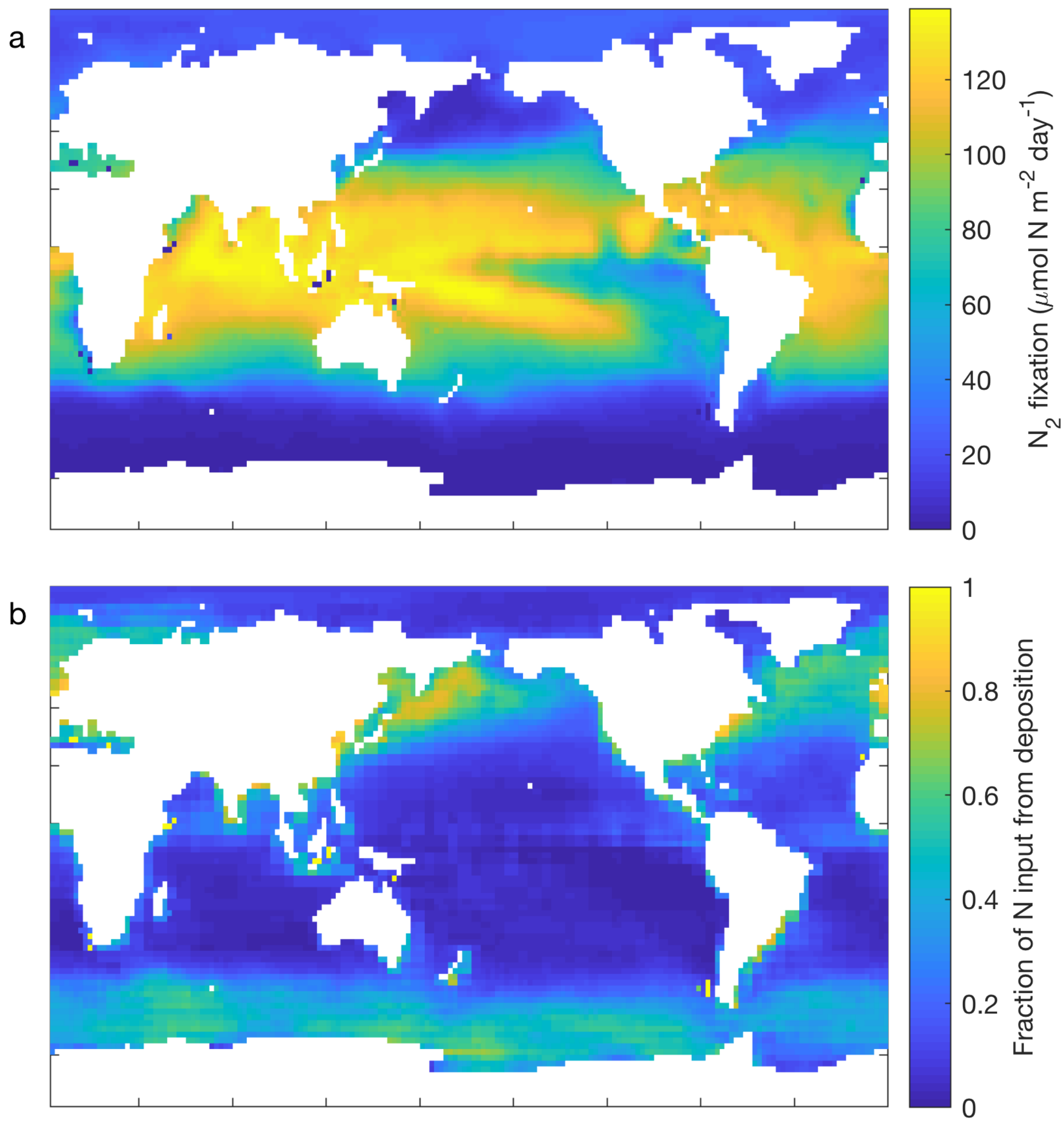

Figure S1

(a) Map of modeled areal N_2 fixation rates. (b) Map of the fraction of N input due to atmospheric deposition of DIN, with the remaining fraction due to N_2 fixation.

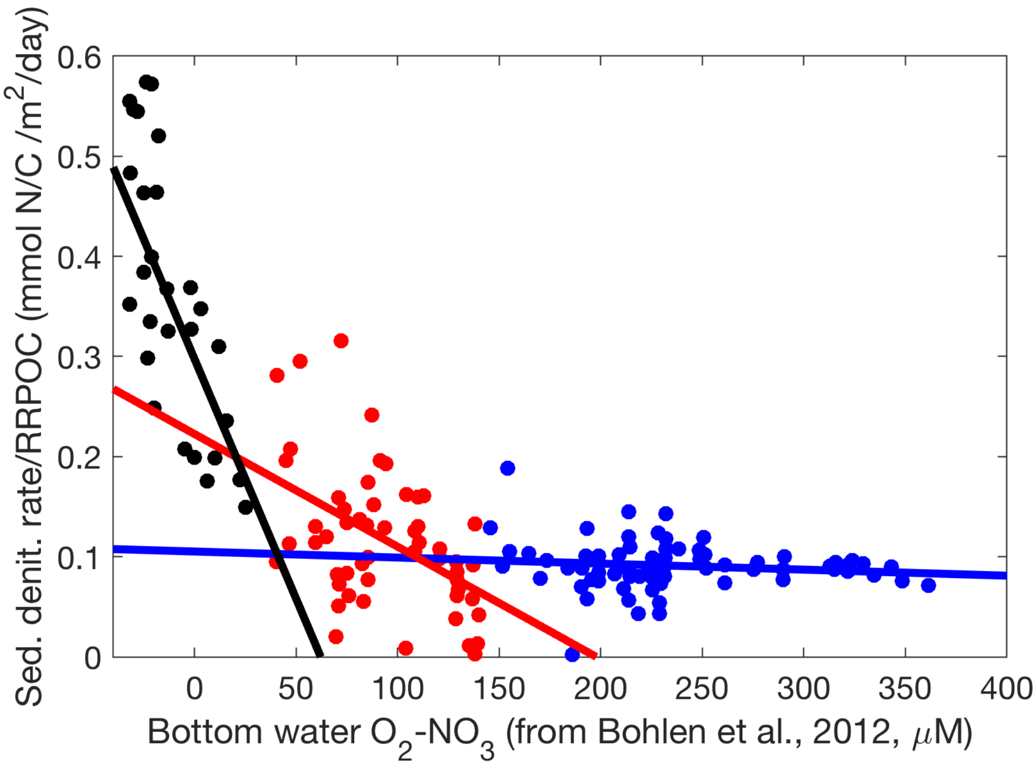

Figure S2. Piecewise division of the transfer function for sedimentary denitrification from Bohlen et al. (2012). In order to incorporate this into our liner model, we split the original non-linear relationship between sedimentary denitrification rate, rain rate of particulate organic carbon (RRPOC), and bottom water ($[O_2] - [NO_3^-]$) into three linear segments with cutoff points in terms of ($[O_2] - [NO_3^-]$). These cutoff points were then converted to $[O_2]$ cutoff points using a relation shown in Figure S2.

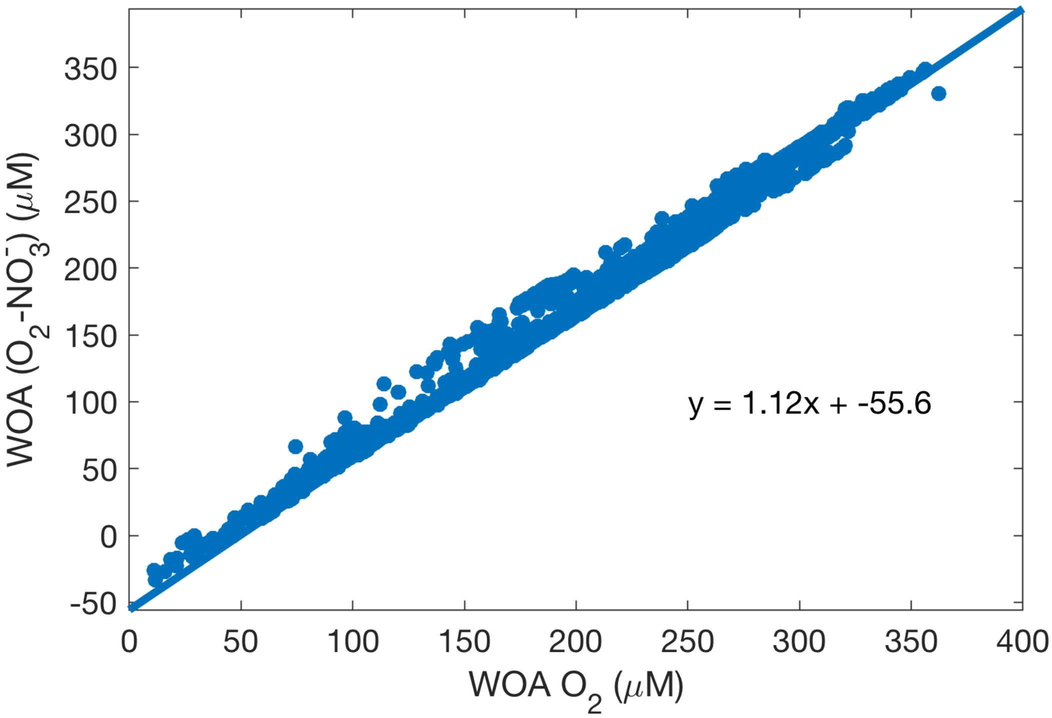

Figure S3. Plot of 2013 World Ocean Atlas [O_2] vs. ([O_2] – [NO_3^-]) (Garcia et al., 2014). In order to express the sedimentary denitrification transfer function cutoff points (Figure S1) in terms of [O_2] rather than ([O_2] – [NO_3^-]), we determined a linear relationship between [O_2] and ([O_2] – [NO_3^-]).

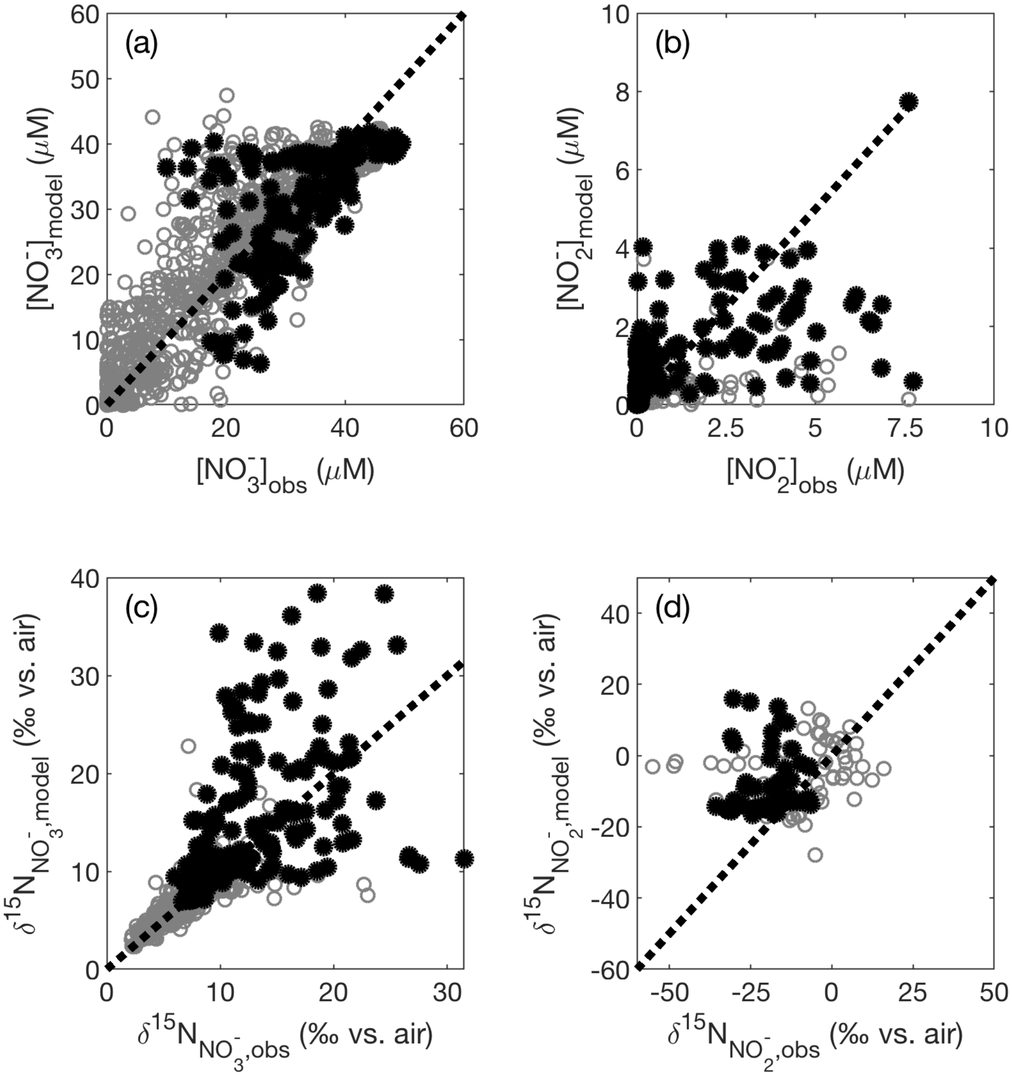

Figure S4. Modeled (a) $[NO_3^-]$, (b) $[NO_2^-]$, (c) $\delta^{15}N_{NO3-}$, and (d) $\delta^{15}N_{NO2-}$ are compared against the corresponding values from the database training set. Shown on each panel is a 1:1 line starting at the origin. Data in black have corresponding $[O_2] < 10$ μM, and data in gray have $[O_2] \geq 10$ μM.

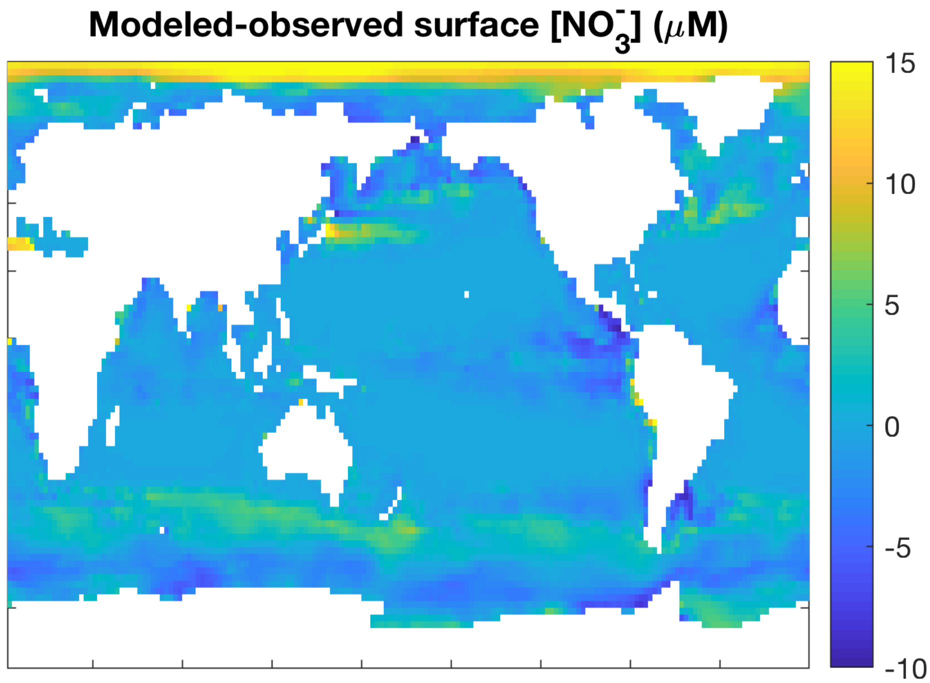

Figure S5. Map showing a comparison between modeled surface [NO_3^-] for the top two model boxes and 2013 World Ocean Atlas [NO_3^-] (Garcia et al., 2014) interpolated to the model grid for the same depths. Areas where the model overpredicts surface [NO_3^-] are shown in yellow, and underprediction is shown in blue.

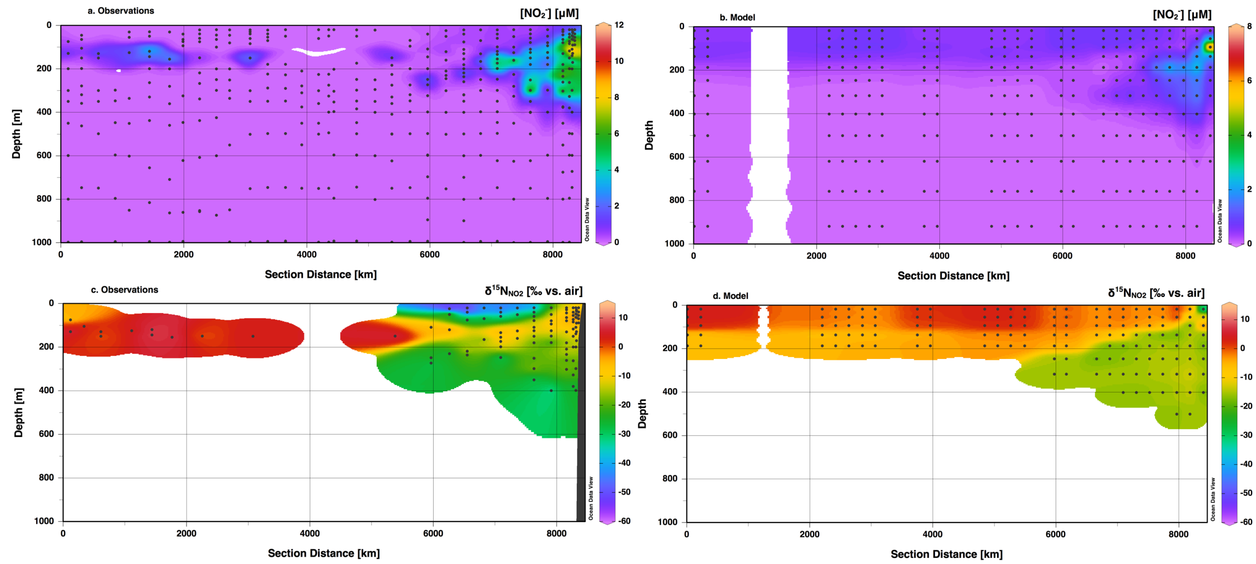

Figure S6. Section profiles of NO_2^- concentrations and isotopes over the GP16 cruise track (panel (a) inset) in the South Pacific. Profiles are presented from east (right) to west (left). Comparison of (a) observed [NO_2^-] to (b) modeled [NO_2^-] is presented over a shortened depth range (0-1000m) to better assess surface and ODZ values where NO_2^- accumulates. GEOTRACES data are from Peters et al. (2018a) and available from BCO-DMO.

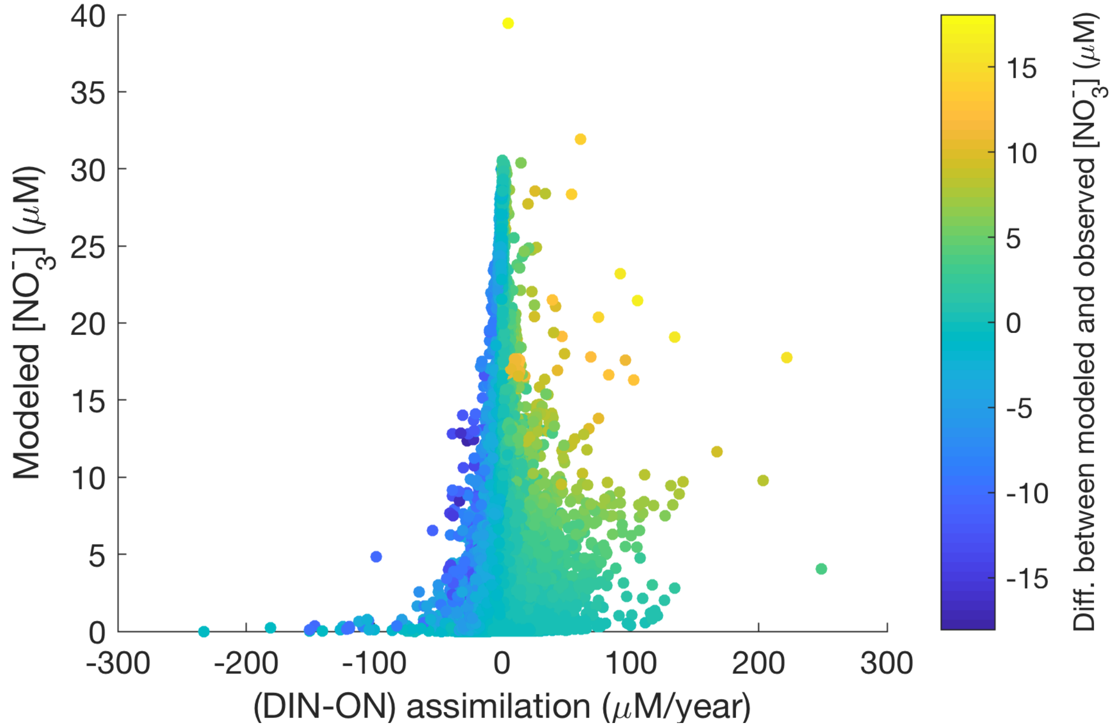

Figure S7. Difference in assimilation rates between the DIN and ON model runs plotted against the modeled [NO_3^-]. Points are colored by the difference between modeled and observed [NO_3^-].

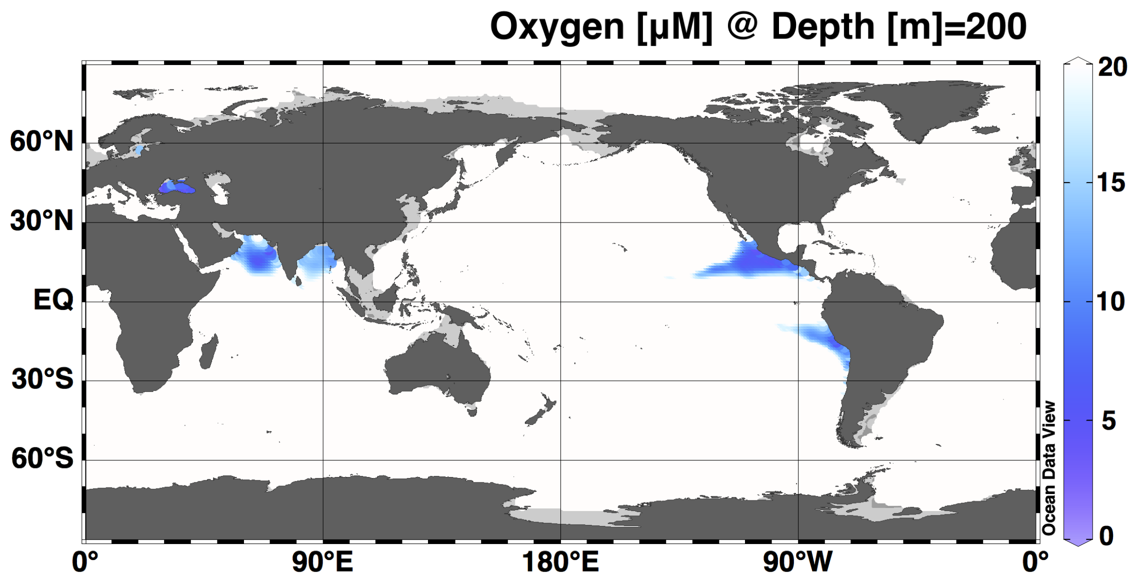

Figure S8. Map of annual average 2013 World Ocean Atlas [O_2] @ 200m depth (Garcia et al., 2014) to demonstrate areas where O_2 is low enough for anoxic processes such as nitrate reduction, nitrite reduction, and anammox. The canonical ODZs are visible in blue: the Arabian Sea, ETNP, and ETSP. Also shown in blue are the Bay of Bengal and the Black Sea.

Global		
N_2 fixation rate (Tg N/yr)	**Method of estimation**	**Reference**
137	Ocean circulation model of P*	Deutsch et al., 2007
110 ± 40[a]	N* observations	Gruber & Sarmiento, 1997
74 (51-110)	Tracer incubations	Luo et al., 2014
131	Global inverse N model	This study
Pacific		
N_2 fixation rate (Tg N/yr)	**Method of estimation**	**Reference**
95	Ocean circulation model of P*	Deutsch et al., 2007
59 ± 14	N* observations	Deutsch et al., 2001
37 (25-56)	Tracer incubations	Luo et al., 2014
67	Global inverse N model	This study
Atlantic		
N_2 fixation rate (Tg N/yr)	**Method of estimation**	**Reference**
20	Ocean circulation model of P*	Deutsch et al., 2007
30.5 ± 4.9	Nitrate isotope mass balance	Marconi et al., 2017
27.6 ± 10	Tracer incubations	Fonseca-Batista et al., 2017
28[a]	N* observations	Gruber & Sarmiento, 1997
13.6 (9.7-19.4)	Tracer incubations	Luo et al., 2014
32	Global inverse N model	This study

a. Extrapolated from N. Atlantic estimate

b. Only from 10˚N-50˚N

Table S1. Global N_2 fixation rate comparisons.

Location and year sampled	**Data types**	**Reference**
ETNP, 2003	$[NO_3^-]$, $[NO_2^-]$, $\delta^{15}N_{NO3-}$, $\delta^{15}N_{NO2-}$	Casciotti and McIlvin, 2007
ETNP, 2012	$[NO_3^-]$, $[NO_2^-]$, $\delta^{15}N_{NO3-}$, $\delta^{15}N_{NO2-}$	Casciotti, unpublished
ETSP, 2011	$[NO_3^-]$, $[NO_2^-]$, $\delta^{15}N_{NO3-}$, $\delta^{15}N_{NO2-}$	Casciotti, unpublished
ETSP, 2013	$[NO_3^-]$, $[NO_2^-]$, $\delta^{15}N_{NO3-}$, $\delta^{15}N_{NO2-}$	Peters et al., 2018

Table S2. New additions to the database originally compiled by Rafter et al. (in prep.).

References

- Bohlen, L., Dale, A. W. and Wallmann, K.: Simple transfer functions for calculating benthic fixed nitrogen losses and C:N:P regeneration ratios in global biogeochemical models, Global Biogeochem. Cycles, 26(3), doi:10.1029/2011GB004198, 2012.
- Casciotti, K. L. and McIlvin, M. R.: Isotopic analyses of nitrate and nitrite from reference mixtures and application to Eastern Tropical North Pacific waters, Mar. Chem., 107(2), 184–201, doi:10.1016/j.marchem.2007.06.021, 2007.
- Deutsch, C., Gruber, N., Key, R. M., Sarmiento, J. L. and Ganachaud, A.: Denitrification and N_2 fixation in the Pacific Ocean, Global Biogeochem. Cycles, 15(2), 483–506, 2001.
- Deutsch, C., Sarmiento, J. L., Sigman, D. M., Gruber, N. and Dunne, J. P.: Spatial coupling of nitrogen inputs and losses in the ocean, Nature, 445(7124), 163–167, doi:10.1038/nature05392, 2007.
- Fonseca-Batista, D., Dehairs, F., Riou, V., Fripiat, F., Elskens, M., Deman, F., Brion, N., Quéroué, F., Bode, M. and Auel, H.: Nitrogen fixation in the eastern Atlantic reaches similar levels in the Southern and Northern Hemisphere, J. Geophys. Res. Ocean., 122(1), 587–601, doi:10.1002/2016JC012335, 2017.
- Garcia, H. E., Boyer, T. P., Locarnini, R. A., Antonov, J. I., Mishonov, A. V, Baranova, O. K., Zweng, M. M., Reagan, J. R. and Johnson, D. R.: World Ocean Atlas 2013. Volume 3: dissolved oxygen, apparent oxygen utilization, and oxygen saturation, NOAA Atlas NESDIS 75, 3, 27, 2013.
- Garcia, H. E., Locarnini, R. A., Boyer, T. P., Antonov, J. I., Baranova, O. K., Zweng, M. M., Reagan, J. R. and Johnson, D. R.: World Ocean Atlas 2013, Volume 4: Dissolved inorganic nutrients (phosphate, nitrate, silicate), NOAA Atlas NESDIS 76, 4, 27 pp, doi:10.1182/blood-2011-06-357442, 2013.
- Gruber, N. and Sarmiento, J. L.: Global patterns of marine nitrogen fixation and denitrification, Global Biogeochem. Cycles, 11(2), 235, doi:10.1029/97GB00077, 1997.
- Luo, Y. W., Lima, I. D., Karl, D. M., Deutsch, C. A. and Doney, S. C.: Data-based assessment of environmental controls on global marine nitrogen fixation, Biogeosciences, 11(3), 691–708, doi:10.5194/bg-11-691-2014, 2014.
- Marconi, D., Sigman, D. M., Casciotti, K. L., Campbell, E. C., Weigand, M. A., Fawcett, S. E., Knapp, A. N., Rafter, P. A., Ward, B. B. and Haug, G. H.: Tropical dominance of N_2 fixation in the North Atlantic Ocean, Global Biogeochem. Cycles, 31, 1608-1623, doi:10.1002/2016GB005613, 2017.
- Peters, B. D., Lam, P. J. and Casciotti, K. L.: Nitrogen and oxygen isotope measurements of nitrate along the US GEOTRACES Eastern Pacific Zonal Transect (GP16) yield insights into nitrate supply, remineralization, and water mass transport, Mar. Chem., 201, 137–150, doi:10.1016/j.marchem.2017.09.009, 2018.